Steel and Composite Structures, *Vol. 22, No. 1 (2016) 183-201*
DOI: http://dx.doi.org/10.12989/scs.2016.22.1.183

Effect of stiffeners on failure analyses of optimally designed perforated steel beams

Ferhat Erdal*

Department of Civil Engineering, Akdeniz University, 07058, Antalya, Turkey

(*Received April 15, 2016, Revised September 22, 2016, Accepted September 26, 2016*)

Abstract. Perforated steel beams can be optimised by increased beam depth and the moment of inertia combined with a reduced web thickness, favouring the use of original I-section beams. The designers are often confronted with situations where optimisation cannot be carried out effectively, taking account of the buckling risk at web posts, moment-shear transfers and local plastic deformations on the transverse holes of the openings. The purpose of this study is to suggest solutions for reducing these failure risks of tested optimal designed beams under applying loads in a self-reacting frame. The design method for the beams is the hunting search optimisation technique, and the design constraints are implemented from BS 5950 provisions. Therefore, I have aimed to explore the strengthening effects of reinforced openings with ring stiffeners, welded vertical simple plates on the web posts and horizontal plates around the openings on the ultimate load carrying capacities of optimally designed perforated steel beams. Test results have shown that compared to lateral stiffeners, ring and vertical stiffeners significantly increase the load-carrying capacity of perforated steel beams.

Keywords: perforated steel beams; effect of stiffener; load carrying capacity; optimum design; failure modes of beams

1. Introduction

During the past half-century, there has been an increase in the use of perforated beams in exploring steel construction solutions. In addition to the increase in resistance, the use of these beams allows a new architectural expression (Altifillisch *et al*. 1957, Toprac and Cooke 1959, Sherbourne 1966 and Bazile and Texier 1968). Perforated steel beams are used as primary or secondary floor beams to achieve long spans and service integration. The sophisticated design and profiling process provides them with greater flexibility in beam proportioning for strength, depth, size and location of holes. This flexibility goes together with the functionality of allowing mechanical installations to pass through the openings. The criterion of satisfactory performance at the service limit requires adequate flexural rigidity to reduce deformations and vibrations. The lightweight appearance of beams with openings, combined with their high strength, never ceases to inspire designers to new structural forms. There are two common types of open perforated steel beams: beams with hexagonal openings, also called castellated beams, and beams with circular openings, referred to as cellular beams. In terms of structural performance, the operation of

*Corresponding author, Assistant Professor, Ph.D., E-mail: eferhat@akdeniz.edu.tr

http://www.techno-press.org/?journal=scs&subpage=6 ISSN: 1229-9367 (Print), 1598-6233 (Online)

splitting and rewelding processes for both beams increases the overall beam depth, moment of inertia and section modulus of the original rolled beam, while reducing the overall weight. Perforated steel beams were first used as a castellated beam version in the 1950s. These beams were mostly used in European countries because of the limited ranges of the available steel rolled sections. The labour cost of these countries was also so low during the post-war period (Husain and Speirs 1973, Galambos *et al*. 1975, Kerdal and Nethercot 1980 and Redwood and Zaarour 1996). The emergence of perforated steel beams with circular openings, called cellular beams, was first for architectural application, where exposed steelwork with circular web openings in the beam was considered aesthetically pleasing. While castellated beams require only one cut with a zigzag pattern, these web-expanded beams are formed by double cutting two semi-circular sections along their centreline in the web of a steel I-beam section along the length of the span. Steel cellular beams invariably produce a more efficient and economical solution than castellated beams by virtue of their flexible geometry. Although the profile for any castellated beam section is standard or fixed, the finished depth, diameter and spacing of holes in cellular beams are completely flexible (Arcelormittal 2010). Steel cellular beams were first used in full-scale destructive tests to confirm structural integrity and design criteria at Bradford University, under the supervision of the Steel Construction Institute (SCI) (Lawson 1988). After several tests, web post buckling was described as the failure mode for cellular beams. Afterwards, evaluation of the results was performed of the design methods for web beams, and analytical studies were undertaken using non-linear finite element analysis to seek the capacity of the web posts and the upper and lower tees. Then, design for simply supported steel and composite cellular beams as used in structures was introduced by Ward (1990). The investigation of the vierendeel mechanism in steel beams with circular web openings based on analytical and numerical studies was presented by Chung *et al*. (2001). The behaviour of these beams has been described, and the flexural, local, web-post strengths and bending modes of non-composite and composite cellular beams have also been derived from the parametric study involving detailed finite element analysis. Later, the stress distribution around the holes of cellular beams under load combinations was investigated by Dinehart *et al*. (2004). The main objective of this study was to describe the critical location around a typical circular cell under load conditions. Then, the effect of asymmetry in the shape of the cross-sectional design of composite asymmetric cellular beams was reported by Lawson (2006). Later, in addition to an overview of cellular beams, the stress distribution around the web openings and the effect of cope geometry on the failure of cellular beams were studied by Hoffman *et al*. (2006). After that, an investigation of vierendeel failures of web-expanded beams with hexagonal and elongated web openings was presented by Wang *et al*. (2014) and Panedpojaman *et al*. respectively (2013 and 2015). Finally, an experimental study on long-spanning composite cellular beams under distributed and shear loadings was presented by Sheehan *et al*. (2016). In all these studies, the ultimate load capacities and failure modes of these beams were examined with fixed parameters.

This experimental study suggests that the strengthening effects of different stiffeners on the ultimate load carrying capacities of optimally designed perforated steel beams with design variables can be tested in a self reacting frame. The tests were carried out on eight full-scale steel cellular beams. There are two different types of NPI_CB_200 and NPI_CB_240 I-section beams; four tests were conducted for each specimen. These optimally designed beams, which have beginning span lengths of 5 m, are subjected to point load acting in the middle of the upper flange. The tested cellular beam specimens were optimised using one recent stochastic search technique, called the hunting search algorithm (Oftadeh *et al*. 2010). This meta-heuristic search algorithm

was successfully applied to the optimum design problems of perforated steel beams, where the design constraints were implemented from *BS5950* provisions (British Standards 2000). In this formulation, the sequence number of the I-section beam, the diameter of the openings, and the total number of holes in the cellular beam were treated as design variables.

2. The design of perforated steel beams

The ultimate state design of a steel beam necessitates checking its strength and serviceability. The computation of the strength of a beam with various web openings is determined by considering the interaction of flexure and shear at the openings. Consequently the constraints to be considered in the design of a cellular beam include the displacement limitations, overall beam flexural capacity, beam shear capacity, overall beam buckling strength, web post flexure and buckling, vierendeel bending of upper and lower tees, local buckling of compression flange, and practical restrictions for cell diameter and the spacing between cells. The design process of a cellular beam consists of checks such that the aforementioned failure modes do not occur. The design procedure given here is taken from The Steel Construction Institute (SCI) Publication No: 100 titled "*Design of Composite and Non-composite Cellular Beams*" (Ward 1990). The design methods are consistent with *BS5950* parts 1 and 3 (British Standards 2000). The basic geometry and notation used for the mentioned beams are shown in Fig. 1.

Although the diameter of the holes and spacing between their centres are left to the designer to select, the following ratios are required to be observed

$$1.08 < \frac{S}{D_0} < 1.5 \tag{1}$$

$$1.25 < \frac{H_S}{D_0} < 1.75 \tag{2}$$

Where; D_0 is the diameter of holes, H_s is the final depth of beam, S is distance between centrals of holes, t_w is the web thickness, b_F and t_F are the width and the thickness of the flange, respectively.

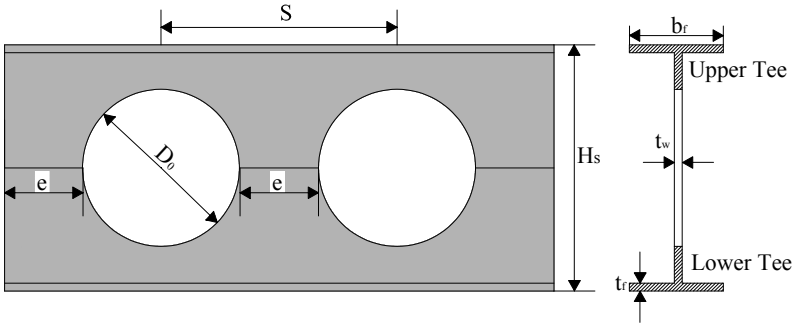

Fig. 1 Design variables for a cellular beam

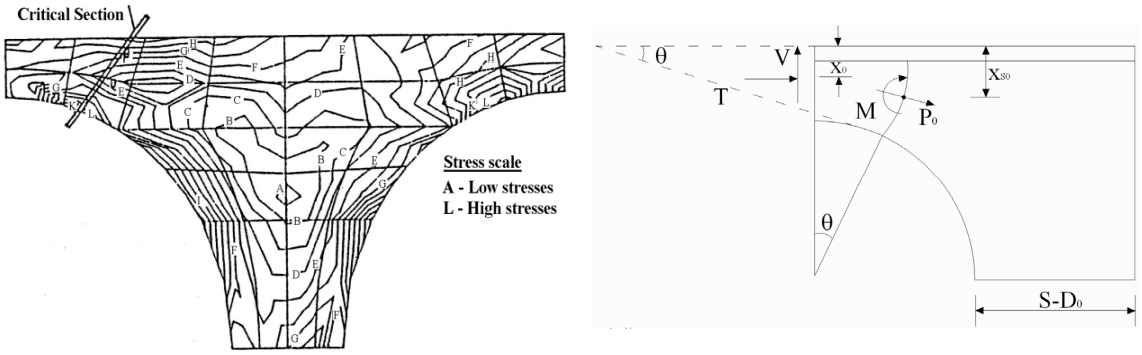

(a) Stress contours due to vierendeel bending (b) Olander's curved beam approach

Fig. 2 Stress contours due to vierendeel bending and Olander's curved beam approach

2.1 Vierendeel bending of upper and lower tees

Further non-linear finite element analyses, using the model as that used to investigate web post buckling demonstrated that final failure is dominated by web post failure for low axial force in the tee and vierendeel failure for high axial force in the tee. Fig. 2(a) shows a Von Mises stress pattern for vierendeel bending close to failure. The transfer of shear forces across a single web opening causes secondary bending stresses. The critical vierendeel bending stresses around the hole may be calculated using Olander's approach (Ward 1990). Olander utilises a circular section for the position of the critical section; the ultimate resistance of the tees is shown in Fig. 2(b).

The interaction between vierendeel bending moment and axial force for the critical section in the tee should be checked as follows

$$\frac{P_O}{P_U}+\frac{M}{M_P}\le 1.0 \tag{3}$$

$$P_O = T\cos\theta-\frac{V}{2}\sin\theta \tag{4}$$

$$M = T\left(x_{S0}-x_0\right)+\frac{V}{2}\left(\frac{H_S}{2}-x_{S0}\right) \tag{5}$$

Where P_y is the design strength of steel, M_p is the nominal moment strength, T is the axial force, V is the shear force, P_0 and M define the force and the moment on the section, respectively. P_u is equal to area of critical section x P_y, M_p is calculated as the plastic modulus of critical section x P_y in plastic sections or elastic section modulus of critical section × P_y for other sections.

2.2 Beam shear capacity

It is necessary to check two shear failure modes in cellular beams. The first one is the vertical shear capacity check in the beam. The sum of the shear capacities of the upper and lower tees gives the vertical shear capacity of the beam. The factored shear force in the beam should not

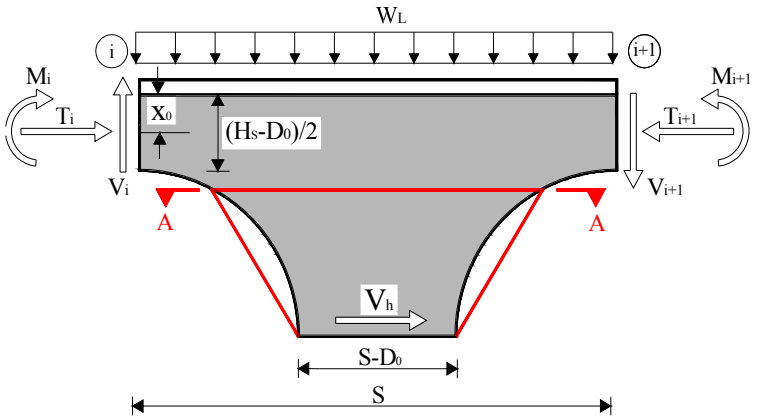

Fig. 3 Horizontal shears in web post of a cellular beam

exceed P_{VY}

$$P_{VY} = 0.6\, P_Y \left(0.9\, A_{WUL}\right) \tag{6}$$

The other is the horizontal shear check failure. The horizontal shear is developed in the web post due the change in axial forces in the tee as shown in Fig. 3. The horizontal shear capacity in the web post of beam should not exceed P_{VH} where

$$P_{VH} = 0.6\, P_Y \left(0.9\, A_{WP}\right) \tag{7}$$

2.3 Flexural and buckling strength of web-post

In this dissertation study the compression flange of the cellular beam is assumed to be sufficiently restrained by the floor system it is attached to. Hence the overall buckling strength of non-composite cellular beam is omitted from the design consideration. Instead the web post flexural and buckling capacity is checked using the Eq. (8)

$$\frac{M_{MAX}}{M_E} = \left[C_1 \left(\frac{S}{D_0} \right) - C_2 \left(\frac{S}{D_0} \right)^2 - C_3 \right] \tag{8}$$

Where M_{MAX} is the maximum allowable web post moment and M_E is the web post capacity at section *A*-*A* of Fig. 3 which is computed as elastic section capacity of design strength of steel. C_1, C_2 and C_3 are constants.

2.4 Classification of perforated beams

The computation of the nominal moment strength of a laterally supported beam necessitates first the classification of the cellular beam. The beam can be plastic, compact, non-compact or slender according to BS5950 provisions. In compact sections, local buckling of the compression flange and the web does not occur before the plastic hinge develops in the cross section. On the

Table 1 Limiting width to thickness ratios

Type of element	Plastic	Compact	Semi-compact
Outstand element of compression flange	$b_f / 2t_f \leq 8.5\epsilon$	$b_f / 2t_f \leq 9.5\epsilon$	$b_f / 2t_f \leq 15\epsilon$
For web, with neutral axis at mid-depth	$(H_S - 2t_f)/t_w \leq 79\epsilon$	$(H_S - 2t_f)/t_w \leq 98\epsilon$	$(H_S - 2t_f)/t_w \leq 120\epsilon$

other hand in compact sections, the local buckling of compression flange or web may occur after the first yield is reacted at the outer fiber of the flanges. Classification of I-shaped sections is carried out according to Table 1 of BS5950 which is repeated below.

The moment capacity of beams for plastic or compact sections and semi-compact sections is calculated in Eqs. (9) and (10). In these equations; S_x is the plastic modulus and Z_x is the elastic modulus of section about relevant axis. In Eq. (11), $\mathcal{E}$ defines a constant in connection with limiting with to thickness ratios. λ_F given in Eq. (12) is slenderness ratio for I-shaped member flanges. Eq. (13) describes, λ_W, slenderness ratio for beam web, in which H plus allowance for undersize inside fillet at compression flange for rolled I-shaped sections shown in Eq. (14), where d is the overall depth of the section. H / t_w is readily available in I-section properties table.

$$M_{P(plastic)} = P_Y \times S_x \tag{9}$$

$$M_{p(elastic)} = P_Y \times Z_x \tag{10}$$

$$\varepsilon = \left(275 / P_Y\right)^{1/2} \tag{11}$$

$$\lambda_F = b_F / 2t_F \tag{12}$$

$$\lambda_W = H / t_W \tag{13}$$

$$H = d - 2t_F \tag{14}$$

2.5 Deflection of perforated steel beam

The limiting values for deflection of a beam under applied load combinations are given in BS5950, Part 1. According to these limitations the maximum deflection of a perforated steel beam should not exceed span/360. The deflection of perforated steel beam is computed using the virtual work method which is explained in detail in Knowles (1980). Fig. 3 also shows points of inflection at sections i and i + 1. Shear force under applied load combination is distributed equally tees, the axial and horizontal forces in the upper and lower tee are given by

$$T_i = \frac{M_i}{h} \quad \text{and} \quad V_h = \frac{S(V_i + V_{i+1})}{2h} \tag{15}$$

Where; h is distance between the centre of upper and lower tees and S is distance between centrals of holes. The deflection at each point is found by applying a unit load at that point. Iternal forces under a unit load are given by $\overline{V_i}/2$, $\overline{N_i}$, $\overline{T_i}$.

Deflection due to bending moment in tee

$$y_{mt} = 0.091(D_0 / 2)^3 / (3EI_T)(V_i \overline{V_i}) \tag{16}$$

Deflection due to bending moment in web post of beam

$$y_{wp} = \frac{13.15}{Et_w}\left[\log_e\left(\frac{S - 0.9(D_0/2)}{S - 2.0(D_0/2)}\right) + 2\left(\frac{S - 2.0(D_0/2)}{S - 0.9(D_0/2)}\right) - \frac{1}{2}\left(\frac{S - 2.0(D_0/2)}{S - 0.9(D_0/2)}\right)^2 - \frac{3}{2}\right] V_h \overline{V_h} \tag{17}$$

Deflection due to axial force in tee

$$y_{at} = 2S / (EA_T)(T_i \overline{T_i}) \tag{18}$$

Deflection due to shear in tee

$$y_t = 0.45(D_0 / 2) / (GA_{TWEB})(V_i \overline{V_i}) \tag{19}$$

Deflection due to shear in web post

$$y_w = \frac{1.636}{Gt_w} X \log_e\left(\frac{S - 0.9(D_0/2)}{S - 2.0(D_0/2)}\right) V_h \overline{V_h} \tag{20}$$

Where E is the elasticity modulus of steel, I_T is total moment of inertia of beam, G is shear modulus and X is the web post form factor. The total deflection of a single opening under applied load (Eq. (21)) is obtained by summing the deflections computed in Eqs. (16)-(20). On the other hand, the deflection of the castellated beam is calculated by multiplying the deflection of each opening by the total number of openings in the beam as given from Toprac and Cooke (1959).

$$y_T = y_{mt} + y_{wp} + y_{at} + y_t + y_w \tag{21}$$

3. Meta-heuristic search techniques in optimization

The solution methods available among the mathematical programming techniques to obtain optimum results to discrete programming problems are not very efficient for practical use. Fortunately, the emergence of stochastic methods that are based upon the mimicking of paradigms found in nature has changed this situation altogether. The basic idea behind search techniques is to simulate the natural phenomena, such as the cooling process of molten metals through annealing into a numerical algorithm (Kirkpatrick *et al*. 1983), survival of the fittest in genetic algorithms (Goldberg, 1989), flock migration in swarm intelligence (Kennedy *et al*. 2001), shortest path to food source in ant colony optimization (Dorigo and Stützle 2004), best harmony of instruments in harmony search technique (Geem and Lee 2004), accelerations of charge particles in charged system search (Kaveh and Talatahari 2010), and looking for a prey in hunting search algorithm (Oftadeh *et al*. 2010) that is automated by nature to achieve the task of optimization of its own.

The design algorithms developed using search techniques are very effective for global search owing to their capability of the finding optimum solutions in the search space at an affordable time (Hasançebi *et al*. 2010). A hunting search algorithm is suggested in this paper as an efficient algorithm for solving perforated steel beams problems. The robustness of the proposed algorithm is numerically tested with design example on size optimum design of mentioned beams.

3.1 Hunting Search Algorithm (*HSA*)

The hunting search method based optimum design algorithm has six basic steps, which are outlined as follows (Oftadeh *et al*. 2010):

3.1.1 Initialising design algorithm and parameters

HGS defines the hunting group size, which is the number of solution vectors in the hunting group; *MML* represents the maximum movement toward the leader, and *HGCR* is the hunting group consideration rate, which varies between 0-1.

3.1.2 Generation of hunting group

On the basis of the number of hunters (*HGS*), the hunting group is initialised by selecting a random sequence number of steel sections (I_i) for each group.

$$I_i = INT\left[I_{\min} + r\left(I_{\max} - I_{\min}\right)\right] \quad i = 1,....,n \tag{22}$$

Where; the term r represents a random number between 0-1, $I_{\min}$ is equal to 1 and $I_{\max}$ is the total number of values in the discrete set respectively. n is number of design variables.

3.1.3 Moving toward the leader

The positions of hunters are generated by moving toward the leader hunter. I_i^L is the position value of the leader for the i-th variable in Eq. (23).

$$I_i' = I_i + r\ MML\left(I_i^L - I_i\right) \qquad i = 1,....,n \tag{23}$$

3.1.4 Position correction-cooperation between hunters

After moving toward the leader, hunters tend to choose another position to conduct the 'hunt' efficiently, i.e., better solutions.

$$I_i^{j'} \leftarrow \begin{cases} I_i^{j'} \in \left\{ I_i^{1'},\ I_i^{2'},...,I_i^{HGS} \right\} & \text{with probability HGCR} \\ INT\left(I_i^{j'} = I_i \pm Ra\right) & \text{with probability (1 - HGCR)} \end{cases} \tag{24}$$

3.1.5 Reorganizing the hunting group

Hunters must reorganize to get a new chance for obtaining the global optimum. If the difference between the objective function values obtained by the leader and the worst hunter in the group becomes smaller than a predetermined constant (ε_1) and the termination criterion is not satisfied, then the group reorganized. By employing the Eq. (25), leader keeps its position and the others randomly select positions.

$$I_i' = I_i^L \pm r\left(\max(I_i) - \min(I_i)\right)\alpha(-\beta\ EN) \tag{25}$$

Where; I_i^L is the position value of the leader for the i-th variable, r represents the random number between 0-1, min(I_i) and max(I_i) are minimum and maximum values of variable I_i, respectively, EN refers to the number of times that the hunting group has trapped until this step. α and β are determine the convergence rate of the algorithm.

3.1.6 Termination

The steps of moving toward the leader and reorganizing hunting group are repeated until the maximum number of cycles is reached.

4. Design examples of steel perforated beams

In the experimental part of our research, the strengthening effects of vertical, horizontal and ring stiffeners on optimally designed steel cellular beams are tested in a self reacting frame. All specimen tests are conducted in the Structural Engineering laboratory at Akdeniz University. The tested cellular beam specimens are designed using the hunting search optimisation method, as explained in the previous section. The design steps of cellular beams are summarised very briefly here; detailed implementation specifics can be found in Erdal *et al*. (2011, 2013).

4.1 NPI_200 and NPI_240 based steel perforated beams with 5-m span

Simply supported cellular beams with a span of 5 m are subjected to concentrated loads; live loads of 50 kN for NPI_200 based beam and 80 kN for NPI_240 based beam shown in Fig. 4.

The allowable displacement of the beam space under the live-load is limited to 14 mm. The modulus of elasticity is taken as 205 kN/mm^2 and the design strength for Grade 37 of steel is 235 kN/mm^2. For this simply supported beam, the hunting group size (*HGS*) is taken as 40. The hunting group considering rate (*HGCR*) is selected as 0.30, while the maximum movement toward the leader (*MML*) is considered as 0.005 on the basis of the empirical findings by Oftadeh *et al*. (2010). The maximum number of searches was set to 10,000 for this example. The optimum designs of the cellular beams are carried out by the algorithm presented, and the optimum results obtained are given in Table 2.

These optimum designs are determined after 10,000 cycles, and the minimum weights of both beams are 128.4 kg and 174.9 kg, respectively. The hunting search algorithm selects NPI-200

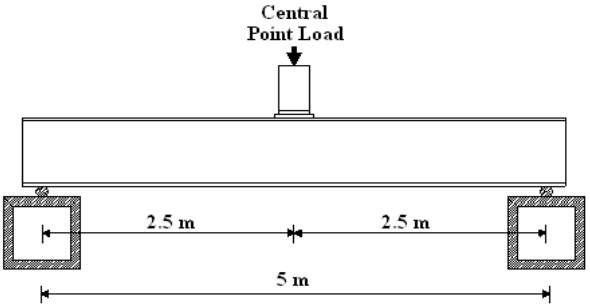

Fig. 4 Typical cross section of beam with 5-m for NPI-200 and NPI-240 Sections

Table 2 Optimum solutions of 5-m span intermediate steel perforated beams

Hunting search algorithm				
Section design (NPI)	Diameter of hole	Number of holes	Max. strength ratio	Minimum weight (kg)
NPI_200_SPB	**217**	**18**	**0.98**	128.4
NPI_240_SPB	**290**	**13**	**0.99**	174.9

profile section, 18 circular holes and 217 mm for the hole diameter and NPI-240 profile section, and 13 circular holes and 290 mm for the hole diameter, respectively. The controlling interaction ratios of NPI-200 based steel cellular beam are 0.98 for bending moment, 0.78 for web-post buckling and 0.62 for horizontal shear. On the other hand, the controlling interaction ratios of NPI-240 based cellular beam are 0.99 for bending moment, 0.71 for web-post buckling and 0.57 for horizontal shear. These results clearly reveal the fact that, in both beams, bending moment constraints are dominant. More detail about the optimisation process of cellular beams is given in (Erdal *et al*. 2011).

5. Experimental program

The tests were carried out on eight full-scale non-composite cellular beams to find out the strengthening effects of reinforced openings with ring stiffeners, welded vertical simple plates on the web posts and horizontal plates around the openings on the ultimate load carrying capacities of optimally designed open web-expanded steel beams. The manufacturing processes of reinforced beams are demonstrated in Fig. 5. All of the beams were subjected to a single concentrated load therefore local failure types (web-post buckling and vierendeel bending) were occurred in the experiments. The reason for web buckling is web thickness, the ratio of pitch opening and hole

Fig. 5 The fabrication process of perforated beams with stiffeners

Table 3 Dimensional Properties of NPI_200 and NPI_240 based Cellular Beams

Section designation	NPI_200_SPB (mm)	NPI_240_SPB 240 (mm)
H_s	296.2	369.8
b_f	90	106
t_f	11.3	13.1
t_w	7.5	8.7
D_0	217	290
S	57.6	87.5
L	4999.6	4999.5
t_{stif}	7.5	8.7
h_{stif}	273.6	363.6
l_{stif}	296.2	369.8
d_{stif}	1860.1	2283.4

diameter. When the load applies above the holes similar to this NPI_240 beams case, vierendeel bending effect has occurred on the beams in addition to web buckling.

5.1 Test specimens and loading arrangement

The two different steel sections adopted were the *NPI_CB_200* and *NPI_CB_240* of steel grade S235, with web opening diameters, D_0, equal to 0.73 and 0.78 times the beam section depths, respectively. These optimally designed beams that have preliminary span lengths of 5 m are subjected to a point load acting at the mid-span. The dimensional properties of these steel perforated beams are reported in Table 3.

All steel cellular beam specimens are placed on simple supports at both ends. During the optimisation process of cellular beams according to *BS5950* specifications, lateral movement is completely assumed to be blocked. For this purpose, a pair of lateral supports is provided at the end of each beam, and one more lateral bracing is integrated into the middle part of the test beams to prevent lateral movement along the span on these beams in the experimental study. The simply

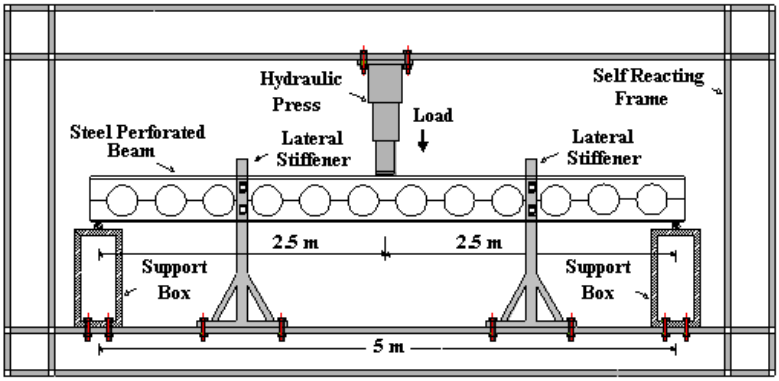

Fig. 6 The demonstration of optimal designed test beams in a self reacting frame

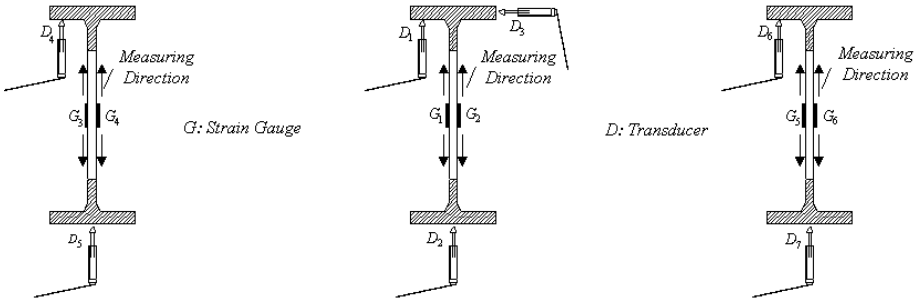

(a) One-quarter of beam (b) Mid-span of beam (c) Three-quarter of beam

Fig. 7 Demonstration of transducers and strain gauges on beam

supported steel cellular beams are tested under the action of a concentrated load. The load is provided by a hydraulic jack reacting on the laboratory floor and aligned equally on each side of the beam. The canister-type load cell used for the experiments is calibrated before any testing procedure took place. An illustration of test setup and one of these specimen cellular beams are given in Fig. 6.

To record the overall displacements of the cellular beams, seven transducers are mounted on the test specimens. Six are placed at one-quarter mid-span and three- quarter of the test beam, respectively. The last transducer is placed at the upper flange of the beam to record lateral displacement. Six strain gauges are also located on both sides of the web at both web openings. The gauges are used to measure the compressive and tensile surface strains of the web-expanded beams shown in Fig. 7. For each test, the adjustment of loading rod positions was applied carefully to prevent eccentric loading.

The main focus of the experiment is to investigate the strength development of steel cellular beams based on different types of stiffeners, and to observe which type of failure would take place after the compression tests on these beams. The results of the reinforced steel beams were directly compared to those of steel beams without stiffeners.

5.2 Effect of stiffeners on NPI_200 Section Steel perforated beams

Four optimally designed cellular beams with 18 openings fabricated from *NPI_200* sections are tested to find out the strengthening effects of reinforced openings with ring stiffeners, welded vertical simple plates on the web posts and horizontal plates around the openings on the ultimate load carrying capacities of optimally designed open web-expanded steel beams. The thicknesses of all stiffeners were selected as 7.5 mm the other way around the web thickness of the original *NPI_200* beam. The lengths of the lateral (l_{stif}), vertical (h_{stif}) and ring stiffeners (d_{stif}) are taken as the same dimensions as the diameter, web height and circumference, respectively.

The failure of NPI_200 based steel cellular beam without stiffeners (having achieved its ultimate load: F_{ult} = 77.11 kN) under directly applied concentrated loading over a web-post is defined as web-post buckling and is illustrated in Fig. 8(a). One of the reasons for this type of failure is the web geometries of these expanded beams. Another reason for web buckling is horizontal shear in the web-post of these tested beams, due to double-curvature bending over the depth of the web-post. The first inclined edge of the opening is stressed in tension and the other edge of the hole in compression, all of which results in a twisting effect of the web post with depth.

(a) *NPI-200* section without stiffener

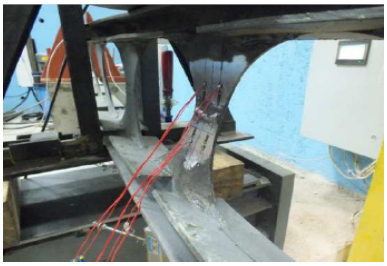

(b) *NPI-200* section with lateral stiffener

(c) *NPI-200* section with ring stiffener

(d) *NPI-200* section with vertical stiffener

Fig. 8 Experimental tests on *NPI-200* based steel perforated beams

Table 4 Ultimate Load Carrying Capacities of Stiffeners on NPI_200 Sections

Type of stiffener	Without stiffener	Lateral stiffener	Vertical stiffener	Ring stiffener
Ultimate loads	77.11 kN	83.82 kN	89.26 kN	91.13 kN
Maximum deflection	51.66 mm	46.71 mm	45.83 mm	42.57 mm
Failure type	Web-post buckling	Web-post buckling	Web-post buckling	Web-post buckling

Vertical displacements on the middle part of the upper and lower flanges of the beams are displayed in Fig. 9.

The maximum deflection values of NPI_200 section based steel perforated beams are shown in Table 4 in more detail.

Lateral displacement is not shown in the load-deflection graph, because the lateral movement values can be neglected, as they are very small. The reason for web buckling is web thickness, the ratio of pitch opening and hole diameter. When the lateral stiffeners are placed on the beam, the load carrying capacities of the *NPI_200*-based steel cellular beam turn out to be 83.82 kN; 8.7% tougher than the original cellular beam demonstrated in Figure 8b. It was observed that the same beam failed under the applied value of 89.26 kN after the vertical stiffeners were provided among the holes. This means that the strength of *NPI_200* based steel cellular beam increases approximately by 12.15 kN after the vertical stiffeners are provided among the holes (Fig. 8(c)). It can be also seen from Fig. 9 that the steel cellular beams failed at 91.13 kN, the maximum load capacity, when all the openings of beam were reinforced with ring stiffeners shownn in Fig. 8(d).
The effect of stiffener's type on the ultimate load carrying capacities of steel cellular beams is demonstrated in Fig. 9 in more detail. The ultimate test loads were reported as the ultimate loads obtained during the experiments; the measured deflection values under these loads and failure types are also shown in Table 4.

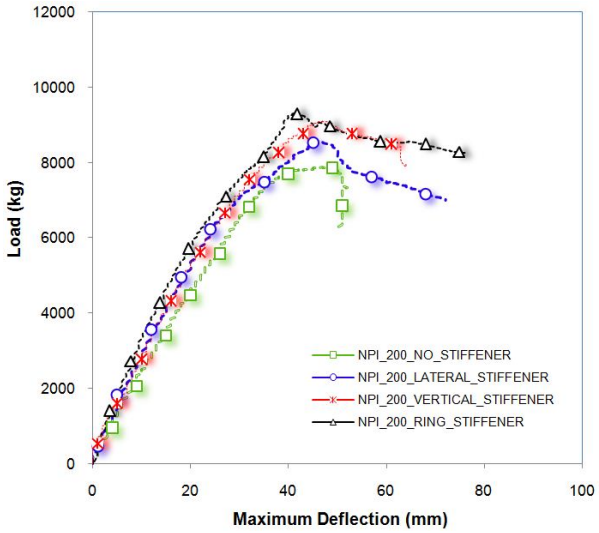

Fig. 9 Load-Deflection Graphic for NPI-200 Section Beams

(a) *NPI-240* section without stiffener

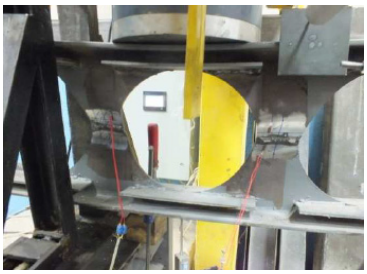

(b) *NPI-240* section with lateral stiffener

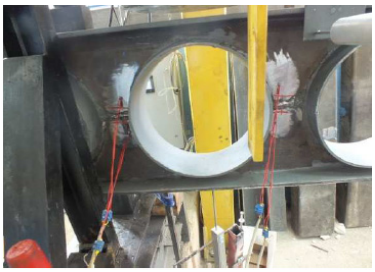

(c) *NPI-240* section with ring stiffener

(d) *NPI-240* section with vertical stiffener

Fig. 10 Experimental tests on NPI-240 based steel perforated beams

Table 5 Ultimate load carrying capacities of stiffeners on NPI_200 sections

Type of stiffener	Without stiffener	Lateral stiffener	Vertical stiffener	Ring stiffener
Ultimate loads	113.02 kN	128.97 kN	134.24 kN	138.13 kN
Maximum deflection	38.72 mm	55.97 mm	44.36 mm	48.16 mm
Failure type	Vierendeel bending and web buckling	Vierendeel bending and web buckling	Vierendeel bending and web buckling	Vierendeel bending and web buckling

5.3 Effect of stiffeners on NPI_240 Section Steel perforated beams

In the second experimental test of this section, four cellular beams with 13 openings fabricated from NPI_240 beam sections were tested to find out the strengthening effects of the same stiffeners on the ultimate load carrying capacities of optimally designed open web-expanded steel beams. Simple supports and a central single point load were used for all four specimens, as with other tests. The thicknesses of all stiffeners were selected as 8.7 mm: the same as the web thickness of the original *NPI_240* beam. The lengths of the lateral, vertical and ring stiffeners are taken as the same dimensions as the diameter, web height and perimeter of optimised diameter, respectively. The results obtained from the experimental test on the *NPI_240* section-based cellular beam without stiffener demonstrates that the flexural capacity of the upper and lower tees under bending is critical. Because the load is directly applied above the holes, in addition to web buckling, vierendeel bending occurred on the beam. This means that, when load is applied directly over the circular openings, the failure behaviour is controlled by the vierendeel bending mechanism displayed in Fig. 10(a).

It was observed that the *NPI_240*-based cellular beam failed under the applied value of 113.03 kN. Vertical displacements in the middle part of the upper and lower flanges of the beams and lateral movements are shown in Fig. 11. Besides the ultimate loads at which the beams lost their load-carrying ability during the experiments, deflection values and failure types are illustrated in Table 5.

The strength of the *NPI_240*-based cellular beam increases by approximately of 15.94 kN after the lateral stiffeners are welded at the top and bottom of the circular holes shown in Fig. 10(b). When only vertical reinforcements are provided among the circular holes (Fig. 10(c)), the load-carrying capacities of the *NPI_240*-based steel cellular beam turn out to be 128.97 kN. Fig. 11 demonstrates the effect of stiffener's type on the ultimate load-carrying capacities of steel cellular beams. The maximum load-carrying capacity of mentioned perforated beam (F_{ult} = 138.25 kN) was increased by up to 22.3% when reinforced openings were used with ring stiffeners (Fig. 10(d)). Ultimate test loads were also reported as the ultimate loads obtained during experiments; the measured deflection values under these loads are shown in Table 4.

6. Conclusions

This study is the first to focus on the application of the recently developed hunting search algorithm to design steel perforated I-sections. The results showed that proposed method is powerful and efficient in finding the optimum solution of combinatorial structural optimisation problems. Last but not least, the strengthening effects of reinforced openings with ring stiffeners, welded vertical simple plates on the web posts and horizontal plates around the openings, on the ultimate load-carrying capacities of optimally designed perforated steel beams, were interrogated under the action of concentrated loadings in a self-reacting frame. The tests were carried out on eight full-scale perforated steel beams with circular openings. The first two experiments on *NPI_200*- and *NPI_240*-based perforated steel beams without stiffeners failed due to web-post buckling and vierendeel bending, respectively. When the lateral stiffeners were placed on the top and the bottom of the circular openings, the load-carrying capacities of the beams were increased by 8.7% and 14.1%, respectively. Experimental research demonstrated that the load-carrying capacities of the beams after welding of vertical stiffeners among holes increased by 15.8% and 18.7%, respectively. The greatest increase in load-carrying capacity was noted in the beams that

were reinforced with ring stiffeners, reaching up to 18.2% and 22.3%, respectively. This study has shown that compared to lateral stiffeners, ring and vertical stiffeners significantly increase the load-carrying capacity of perforated steel beams. Therefore, steel ring and vertical stiffeners suggest solutions for reducing the failure risks of tested optimal beams under applied loads in a self-reacting frame.

Acknowledgments

This paper is partially based on research supported by the Akdeniz University Research Funding (BAP-2012.01.0102.015), which is gratefully acknowledged.

References

Altifillisch M.D., Cooke, B.R. and Toprac, A.A. (1957), "An investigation of welded open web-expanded beams", *Welding Research Council Bulletin*, **47**, 77-88.

ArcelorMittal Ltd. (2010), *Constructive Solutions*, ArcelorMittal Commercial Sections, Luxembourg. http://www.arcelormittal.com/cellbeam

Bazile, A. and Texier, J. (1968), *Tests on castellated beams*, Constr. Métallique, Paris, France, (Volume 3), pp. 12-25.

British Standards, BS 5950 (2000), Structural Use of Steelworks in Building. Part 1. Code of practice for design in simple and continuous construction, hot rolled sections; British Standard Institution, London, UK.

Chung, K.F., Liu, T.C.H. and Ako, A.C.H. (2001), "Investigation on Vierendeel mechanism in steel beams with circular web openings", *J. Construct. Steel Res.*, **57**(5), 467-490.

Dinehart, D.W., Dionisio, M.C., Hoffman, R.M., Yost, J.R. and Gross, S.P. (2004), "Determination of critical location for service load bending stresses in non-composite cellular beams", *Proceedings of the 17th ASCE Engineering Mechanics Conference*, University of Delaware, Newark, Denmark, June.

Dorigo, M. and Stützle, T. (2004), *Ant Colony Optimization*, A Bradford Book, Massachusetts Institute of Technology, USA.

Dougherty, B.K. (1993), "Castellated beams: A state of the art report", Technical Report; J. SA Inst. Civ. Eng., **35**(2).

Erdal, F., Doğan, E. and Saka, M.P. (2011), "Optimum design of cellular beams using harmony search and particle swarm optimizers", *J. Construct. Steel Res.*, **67**(2), 237-247.

Erdal, F., Doğan, E. and Saka, M.P. (2013), "An improved particle swarm optimizer for steel grillage systems", *Struct. Eng. Mech., Int. J.*, **47**(4), 513-530.

Galambos, A.R., Husain, M.U. and Spin, W.G. (1975), *Optimum Expansion Ratio of Castellated Steel Beams*, Engineering Optimization, London, UK, Vol. 1, pp.213-225.

Gandomi, A.H., Yang, X.S. and Alavi, A.H. (2011), "Mixed variable structural optimization using firefly algorithm", *Comput. Struct.*, **89**(23-24), 2325-2336.

Geem, Z.W. and Kim, J.H. (2001), "A new heuristic optimization algorithm: Harmony search", *Simulation*, **76**(2), 60-68.

Goldberg, D.E. (1989), Genetic algorithms in search, *Optimization and Machine Learning*, Addison Wesley.

Hasançebi, O., Çarbaş, S., Doğan, E., Erdal, F. and Saka, M.P. (2010), "Comparison of non-deterministic search techniques in the optimum design of real size steel frames", *Comput. Struct.*, **88**(17-18), 1033-1048.

Hoffman, R., Dinehart, D., Gross, S. and Yost, J. (2006), "Analysis of stress distribution and failure behaviour of cellular beams", *Proceedings of International Ansys Conference*, Pittsburgh, PA, USA, May.

Husain, M.U. and Speirs, W.G. (1973), "Experiments on castellated steel beams", *J. Am. Weld. Soc., Weld. Res. Suppl.*, **52**(8), 329-342.

Kaveh, A. and Talatahari, S. (2010), "Charged system search for optimum grillage system design using the LRFD-AISC Code", *J. Construct. Steel Res.*, **66**(6), 767-771.
Kennedy, J., Eberhart, R. and Shi, Y. (2001), *Swarm Intelligence*, Morgan Kaufmann Publishers.
Kerdal, D. and Nethercot, D.A. (1984), "Failure modes for castellated beams", *J. Construct. Steel Res.*, **4**(4), 295-315.
Kirkpatrick, S., Gerlatt, C.D. and Vecchi, M.P. (1983), "Optimization by simulated annealing", *Science*, **220**(4598), 671-680.
Knowles, P.R. (1980), *Design of castellated beams for use with BS 5950 and BS 449*, Weldable Structures steel produced to BS: Part 1.
Lawson, R.M. (1988), *Design for Openings in the Webs of Composite Beams*, Steel Construction Institute.
Lawson, R.M. (2006), "Design of composite asymmetric cellular beams and beams with large web openings", *J. Construct. Steel Res.*, **62**(6), 614-629.
Lee, K.S. and Geem, Z.W. (2004), "A new structural optimization method based on the harmony search algorithm", *Comput. Struct.*, **82**(9-10), 781-798.
Oftadeh, R., Mahjoob, M.J. and Shariatpanahi, M. (2010), "A novel meta-heuristic optimization algorithm inspired by group hunting of animals: Hunting search", *Comput. Math. Appl.*, **60**(7), 2087-2098.
Panedpojaman, P. and Thepehadri, T. (2013), "Finite element investigation on deflection of cellular beams with various configurations", *Int. J. Steel Struct.*, **13**(3), 487-494.
Panedpojaman, P., Thepehadri, T. and Limkatanyu, S. (2015), "Novel simplified equations for Vierendeel design of beams with (elongated) circular openings", *J. Construct. Steel Res.*, **112**, 10-21.
Redwood, R.G. and Zaarour, W. (1996), "Web buckling in thin webbed castellated beams", *J. Struct. Eng.* (*ASCE*), **122**(8), 860-866.
Sheehan, T., Dai, X., Lam, D., Aggelopoulos, E., Lawson, M. and Obiala, R. (2016), "Experimental study on long spanning composite cellular beam under flexure and shear", *J. Construct. Steel Res.*, **116**, 40-54.
Sherbourne, A.N. (1966), "The plastic behavior of castellated beams", *Proceedings of the 2nd Commonwealth Welding Conference*, (Volume C2), London, UK, April-May, pp. 1-5.
Toprac, A.A. and Cooke, B.R. (1959), *An Experimental Investigation of Open-web Beams*, Welding Research Council Bulletin, New York, NY, USA.
Wang, P., Ma, Q. and Wang, X. (2014), "Investigation on vierendeel mechanism failure of castellated steel beams with filled corner web openings", *Eng. Struct.*, **74**, 44-51.
Ward, J.K. (1990), *Design of Composite and Non-composite Cellular Beams*, The Steel Construction Institute Publication.

CC

Appendix. Optimum design algorithm

The design of a cellular beam requires the selection of a UB beam from which the cellular beam is to be produced, the selection of circular hole diameter and the spacing between the centres of these circular holes or total number of holes in the beam. As a result, the design variables in the optimum design problem of a cellular beam are selected as the sequence number of a universal beam sections in the standard steel sections tables, the circular hole diameter and the total number of holes. For this purpose a design pool is prepared which consists of list of standard UB beam sections, a list of various diameter sizes and a list of integer numbers starting from 2 to 40 for the total number of holes in a cellular beam. The optimum design problem formulated considering the design constraints explained in the previous sections yields the following mathematical model. Find a integer design vector $\{I\}=\{I_1,I_2,I_3\}^T$ where I_1 is the sequence number of for the UB beam section in the standard steel sections list, I_2 is the sequence number for the hole diameter in the discrete set which contains various diameter values and I_3 is the total number of holes for the cellular beam. Once I_1 is selected, then the UB steel beam designation becomes known and all cross sectional properties of the beam becomes available for the design. The corresponding values to I_2 and I_3 in the design sets makes the hole diameter and the total number of holes known for the cellular beam. Hence the design problem turns out to be minimize the weight of the cellular beam

$$W = \rho A L - \rho\left(\pi\left(\frac{D_0}{2}\right)^2 NH\right) \tag{26}$$

Where W denotes the weight of the cellular beam, ρ is the density of steel. A represents the total cross-sectional area of the universal beam section selected for the cellular beam, L is the span of the cellular beam, D is the diameter of holes and NH is the total number of holes in the cellular beam. The cellular beam is also subjected to number of geometrical and behavioral restrictions as given in Eqns. (27-38). Depending on the values of hole diameters, spacing between the hole centers and the final depth of the beam determined; following geometrical constraints must be satisfied

$$g_1 = 1.08\ D_0 - S \le 0 \tag{27}$$

$$g_2 = S - 1.60\ D_0 \le 0 \tag{28}$$

$$g_3 = 1.25\ D_0 - H_S \le 0 \tag{29}$$

$$g_4 = H_S - 1.75\ D_0 \le 0 \tag{30}$$

In Eqs. (27)-(30), S denotes the distance between centers of holes and H_S is the overall depth of cellular beam. The maximum moment, M_U, under applied load combinations should not exceed the plastic moment capacity M_P of the cellular beam for a sufficient flexural capacity

$$g_5 = M_U - M_P \le 0 \tag{31}$$

It is also required that the shear stresses (V_{MAXSUP}) computed at the supports are smaller than

allowable shear stresses (P_V), the ones at the web openings ($V_{O\,MAX}$) are smaller than allowable vertical shear stresses (P_{VY}) and finally, the horizontal shear stresses ($V_{H\,MAX}$) are smaller than the upper limit (P_{VH}) as formulated in inequalities Eqs. (32)-(34).

$$g_6 = V_{MAXSUP} - P_V \leq 0 \tag{32}$$

$$g_7 = V_{O\,MAX} - P_{VY} \leq 0 \tag{33}$$

$$g_8 = V_{H\,MAX} - P_{VH} \leq 0 \tag{34}$$

The web post flexural and buckling capacity of a cellular beam is also required to be checked as given in inequality Eq. (35). In this expression, the maximum moment ($M_{(A-A)MAX}$) determined at A-A section shown in Fig. 4 should be smaller than the maximum allowable web post moment ($M_{W\,MAX}$)

$$g_9 = M_{(A-A)MAX} - M_{W\,MAX} \leq 0 \tag{35}$$

Inequalities Eqs. (36) and (37) check the interaction between the secondary bending stress and the axial force for the critical section in the tee.

$$g_{10} = V_{TEE} - 0.5\ P_{VY} \leq 0 \tag{36}$$

$$g_{11} = \frac{P_0}{P_U} - \frac{M}{M_P} - 1 \leq 0 \tag{37}$$

Where; V_{TEE} represents the vertical shear on the tee at $\theta = 0$ of web opening, P_0 and M are the internal forces on the web section as shown in Fig. 4. The deflection constraint is imposed such that the maximum displacement is restricted to $L/360$, where y_{MAX} denotes the maximum deflection.

$$g_{12} = y_{MAX} - \frac{L}{360} \leq 0 \tag{38}$$